Electrophosphorescence from iridium complex-doped mesogen-jacketed polymers

Ping Wang, Yutao Chuai, Chunpeng Chai, Fuzhi Wang, Guolin Zhang, Guoping Ge, Xinghe Fan*, Haiqing Guo, Dechun Zou*, Qifeng Zhou*

Beijing National Laboratory for Molecular Sciences, Key Laboratory of Polymer Chemistry and Physics of Ministry of Education, College of Chemistry and Molecular Engineering, Peking University, Beijing 100871, China

Abstract

A mesogen-jacketed polymer P-Ct {poly{2,5-bis[(5-*tert*-butylphenyl)-1,3,4-oxadiazole]styrene}} has been investigated as a host material for IrMDPP [Ir(III)bis(5-methyl-2,3-diphenylpyrazine) (acetyl acetonate)] doped polymer electrophosphorescent device. It was found that the device with P-Ct was more efficient than that with PVK. The maximum luminance and external luminous efficiency can reach 3702 cd/m^2 and 0.83 cd/A, respectively, which were higher than those of device with PVK (1999 cd/m^2 and 0.68 cd/A), which can be partly explained by the more balanced carrier injection and transportation and longer lifetime of excitons in P-Ct−TPD−IrMDPP. It was also found that as the IrMDPP content increased in P-Ct−TPD, the EL spectra color shifts from green-yellow to yellow-orange and were different from PL spectra, which was partly due to the dominating role of direct charge-trapping and recombination in the EL process over the energy-transfer routes.
© 2007 Elsevier Ltd. All rights reserved.

Keywords: Mesogen-jacketed polymers; Electrophosphorescence; Iridium complex

1. Introduction

Polymer light-emitting diodes (PLEDs) have made rapid progress since the first report of polymer light-emitting diodes (LEDs) based on poly(*p*-phenylenevinylene) (PPV) by Burroughes et al. [1] in 1990. However, according to simple spin-pairing statistics, the singlet formation probability in the charge recombination process of fluorescent LEDs is only 25%, this limits further performance enhancement of fluorescent LEDs [2]. A research group in Princeton University have broken through the efficiency limitation by using certain small molecule materials which can make use of triplet states [3]. Since then, electrophosphorescent materials and devices are drawing intensely attention in organic light-emitting device research due to their ability to efficiently harvest both

singlet and triplet excitons, leading to internal quantum efficiency (η_{int}) approaching 100% [4]. The phosphorescent materials used were mainly iridium or platinum complexes with organic ligands, and they were doped as an emissive guest into a host material of the emissive layer. Most of the efficient phosphorescent LEDs were fabricated using small molecule materials as host [5]. However, it is interesting to use polymer as host instead of small molecule materials because polymer materials have better processability and are ease of fabrication based on solution processing techniques and have high possibility in flexible flat panel displays [6].

In order to utilize both Förster and Dexter energy transfer in dye doped polymer LEDs, a proper guest−host system must be selected. In general, host materials should be selected to follow after those that have a higher triplet energy level than that of the guest molecules benefits the energy transfer from the host to the guest while prohibits the energy transfer of triplet excitons from the guest to the host material [4a]. In addition, the charge transporting properties of host materials

are also important. Moreover, there should be large overlap between the emission peaks of the host materials and the absorption spectra of the guest materials, where the energy of the host materials after excitation can be transferred to the guest materials [7].

It is known that PVK is a good hole transporting material with high hole mobility [8] and possesses a large exciton lifetime [4b]. PVK has been widely used as host materials in electrophosphorescent devices. Lee et al. [4b] reported QE_{ext} = 1.9% ph/el and a brightness of 2500 cd/m² for Ir(ppy)₃-doped poly(vinylcarbazole) (PVK) devices with 3-(4-biphenyl)-4-phenyl-5-*tert*-butylphenyl-1,2,4-triazole as a hole-blocking layer. In Gong's work [9], QE_{ext} of 10% ph/el and LE of 36 cd/A were achieved by doping [Ir(DPF)₃] into a blend of PVK with PBD. Kawamura et al. [10] reported polymer electrophosphorescent organic light-emitting diodes using PVK host doped with blue, green, and red phosphorescent cyclometalated Ir(III) complexes with green PHOLED exhibiting η_{ext} = 5.1 ± 0.1%.

P-Ct is a kind of mesogen-jacketed polymer in which mesogenic units are attached laterally to the gravity centers of the main chain without spacers; the main chain of mesogen-jacketed polymers are forced to extend and to take rigid conformation which can avoid aggregation because of high population of both bulky and rigid side groups around the backbone and it is easy to synthesize through common radical polymerization [11]. In addition, P-Ct has good electron transporting properties because of 1,3,4-oxadiazole units in the side group and has high band gaps with HOMO (−6.1 eV) and LUMO (−2.7 eV) [12]. Moreover, P-Ct was thermally stable with high T_g (222 °C) [12].

In this work, we use P-Ct (chemical structure is shown in Fig. 1; M_n = 16.0 × 10⁴, M_w/M_n = 1.45) blended with tetraphenylenebiphenyldiamine (TPD) as the host materials and 0.2–10 wt% IrMDPP (chemical structure is shown in Fig. 1) as the guest to fabricate the device of ITO/PEDOT/P-Ct:TPD:IrMDPP(10 wt%)/BCP/Alq₃/Mg:Ag/Ag. The device showed the better maximum external quantum efficiency (0.28%) and higher light output (3700 cd/m²) than the device of 10 wt% IrMDPP doped into PVK blended with 2-*tert*-butylphenyl-5-biphenyl-1,3,4-oxadiazole (PBD) which was 0.24% and 1999 cd/m², respectively. This work demonstrates that efficient electrophosphorescent light-emitting devices can be

realized with novel electron transport mesogen-jacketed liquid crystalline polymers.

2. Experimental

All solvents, poly(*N*-vinylcarbazole) (PVK), 2-(4-biphenyl)-5-(4-*tert*-butylphenyl)-1,3,4-oxadiazole (PBD), aluminum(III) tris(8-hydroxyquinolinate) (Alq₃), bathocuproine (BCP), tetraphenylenebiphenyldiamine (TPD) and poly(3,4-ethylene dioxythiophene):poly(4-styrenesulphonate) (PEDOT:PSS), were purchased from Aldrich and used as-received. The IrMDPP complex and mesogen-jacketed polymer P-Ct studied here are shown in Fig. 1.

The etched indium−tin oxide (ITO) glass substrate was washed in turn with a substrate-cleaning detergent, deionized water, acetone, and ethanol for 15 min, under ultrasonic condition, and finally treated with UV−ozone for about 25 min. PEDOT was spin-coated on the precleaned ITO substrate at 4000 rpm/min forming about 50 nm thickness and dried by baking in air at 120 °C for 10 h. Then the solution of P-Ct blended with TPD(30 wt%) and IrMDPP(0.2−10 wt%) in chlorobenzene with the concentration of 10 mg/mL was spin-coated through a 0.45 μm Teflon filter. For a comparison, the solution of PVK blended with PBD(30 wt%) and IrMDPP(10 wt%) in chlorobenzene with the concentration of 10 mg/mL was spin-coated through a 0.45 μm Teflon filter. Here, TPD was used to improve the hole transport and PBD was used to improve electron transport. The thickness of the spin-coated film was controlled by regulating the spinning speed. Then the coated ITO was transferred into a deposition chamber with a base pressure of 1 × 10⁻⁶ Torr; Alq₃ and BCP films were evaporated onto the polymer layer. Finally, the Mg:Ag layer as the electrode was evaporated.

Cyclic voltammetry (CV) was performed on a computer-controlled EG&G potential/galvanostat model 283 electrochemical analyzer in a solution of tetrabutylammonium perchlorate (0.1 M) in acetonitrile at a scanning rate of 100 mV/s. The polymer film (P-Ct−TPD−IrMDPP) as a working electrode was coated on a square platinum electrode by casting and then dried in air. Platinum wire was used as a counter electrode, and Ag/AgCl (AgCl was plated on silver wire) electrode was used as a reference electrode. Prior to each series of measurements, the cell was deoxygenated with argon.

All device measurements were carried out in air at room temperature. Absorption spectra were measured using a CARY 1E spectrophotometer of Australian Varian Company, with the wavelength between 190 nm and 900 nm and the width of the spectral band between 0.2 nm and 4.0 nm. Photoluminescence (PL) spectra were obtained using a Hitachi F-4500 luminescence spectrometer. Time-resolved photoluminescence measurements were carried out with Edinburgh Instruments FL900 and nanosecond hydrogen light was used as the excitation source. The samples were measured in air.

The EL spectra were measured with a spectrofluorometer FP-6200 (JASCO). A source-measure unit R6145 (Advantest), multimeter 2000 (Keithley) and luminance meter LS-110 (Minolta) were used for $I−V−L$ measurements. Relative
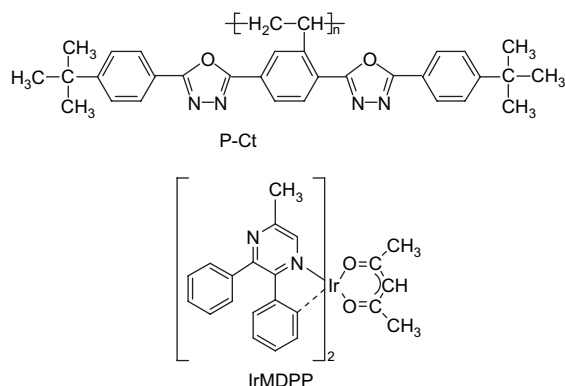

Fig. 1. Chemical structure of P-Ct and IrMDPP.

luminance was directly detected by using a multifunctional optical meter 1835-C (Newport).

3. Results and discussion

To test the Förster energy transfer we first used optical excitation, which generates only singlets [13] in the host. The emission spectrum of the host P-Ct—TPD(30 wt%; excited at 315 nm) and the absorption spectrum of the guest IrMDPP are shown in Fig. 2, the films of host and guest were prepared by spin-coating and drop-casting, respectively. The absorption peak of IrMDPP at 393 nm and 528 nm was attributed to the singlet metal—ligand charge transfer (^{1}MLCT, $\lambda = 393$ nm) and the triplet (^{3}MLCT, $\lambda = 528$ nm) [21]. The partial overlap between the absorption of the IrMDPP at 393 nm and 528 nm and the emission from the polymer fulfills the main requirement for Förster energy transfer from the singlet-excited state in the host to the ^{1}MLCT band of the guest. Fast intersystem crossing to the triplet state of the IrMDPP and subsequent emission from this state are built in features.

The partial overlap between the PL spectrum of P-Ct—TPD and the ^{1}MLCT absorption spectrum of IrMDPP (Fig. 2) implies that the energy transfer from the host to the guest might happen only at a moderate level. In order to test the efficiency of the Förster energy transfer, films consisting of blends of 0.0%, 0.2%, 0.5%, 1.0%, 3.0%, 6.0% and 10% by weight of IrMDPP in P-Ct—TPD(30 wt%) were spin-coated from chlorobenzene solution and excited optically (Fig. 3). As shown by the PL spectra of the spin-coated films of the IrMDPP:P-Ct—TPD blends in different ratios, there existed another broad emission peak of 494 nm from the host P-Ct—TPD(30 wt%) than pure P-Ct, which was attributed to the exciplex formation from P-Ct and TPD [14]. Only when the IrMDPP content was over 1%, the emission from the ^{3}MLCT of the guest can be observed. The emission from the host cannot be completely quenched even with more than 10 wt% of IrMDPP.

We employed the device configuration of ITO/PEDOT/P-Ct—TPD:IrMDPP(0.2—10 wt%)/BCP/Alq$_3$/Mg:Ag/Ag. PEDOT
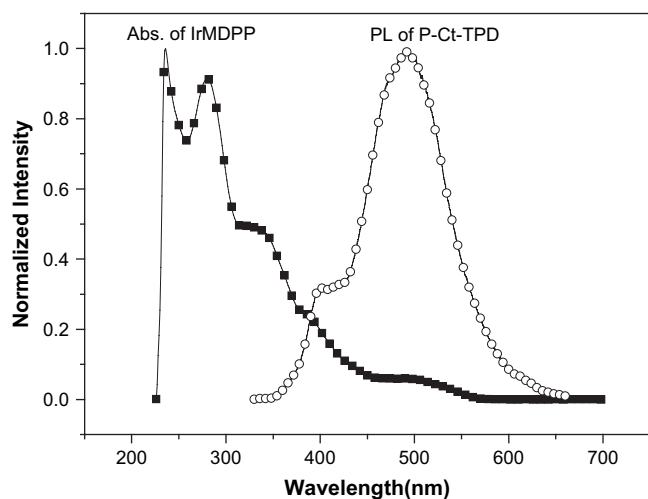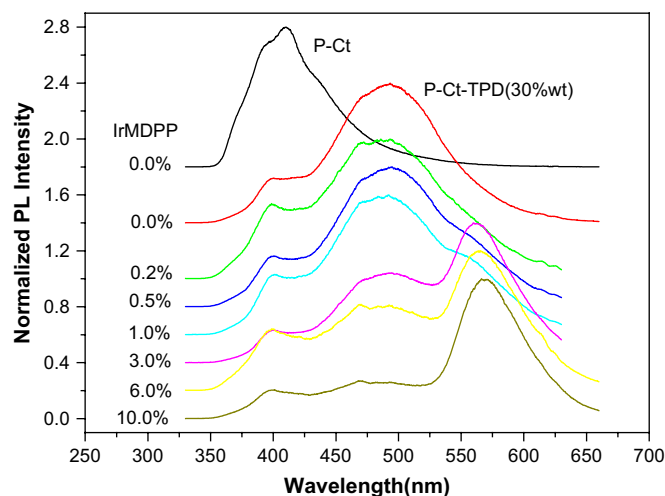

Fig. 3. The photoluminescence spectra of IrMDPP/P-Ct—TPD(30 wt%) films with different doping concentrations of IrMDPP.

was used as hole injection layer and for smoothness. BCP functioned as electron-blocking and exciton-confining layer. The EL spectra corresponding to the LEDs utilizing the blends of IrMDPP—P-Ct—TPD as the emitting layer are shown in Fig. 4. In contrast to the PL spectra, EL spectra show only the guest ^{3}MLCT emission for blends with IrMDPP content over 1%. The dramatic difference between the EL and PL spectra is similar to the dominating role of direct charge trapping and recombination in the EL process over the energy-transfer routes [15]. The main function of the P-Ct—TPD host is to transport the injected carriers efficiently to the IrMDPP trap sites dispersed within the entire EL layer, while the transfer of singlet excitons formed on the polymer chains to the ^{3}MLCT levels via the ^{1}MLCT bridges of the Ir complex only plays a minor role. In order to investigate the charge trapping in the EL process, we measured the HOMO and LUMO energies from CV measurement, and the CV diagram of IrMDPP is given in Fig. 5. The cyclic voltammogram of the
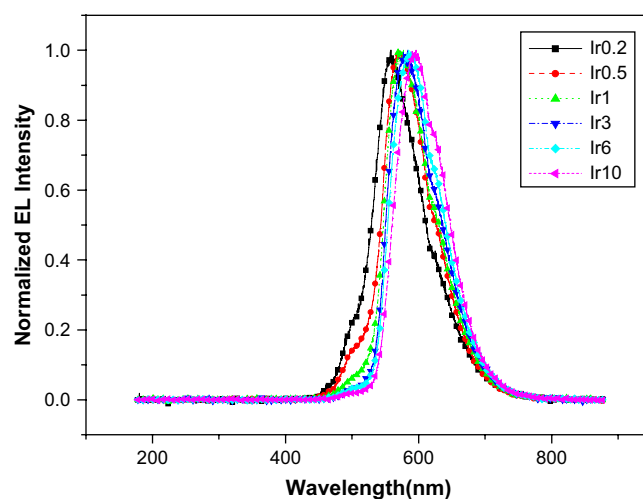

Fig. 2. The normalized absorption spectrum of a neat IrMDPP film and photoluminescence spectrum of P-Ct—TPD(30 wt%).

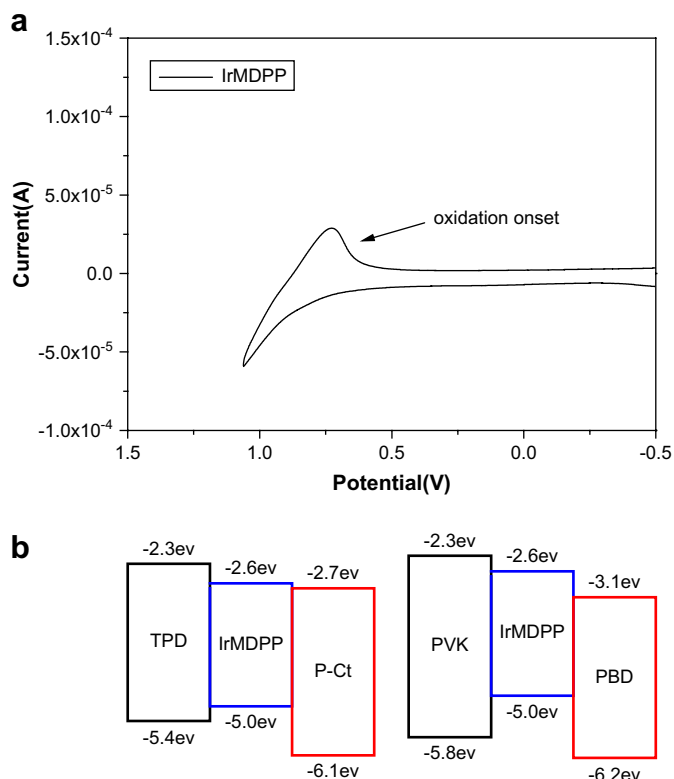Fig. 4. The EL spectra of OLEDs based on different doping concentrations of IrMDPP.

Fig. 5. (a) Cyclic voltammogram of PCt–TPD(30 wt%)–IrMDPP(10 wt%) film measured in acetonitrile in the presence of 0.1 M tetrabutylammonium perchlorate as the supporting electrolyte with a 100 mV/s scan speed. (b) Energy diagrams with device PCt–TPD(30 wt%)–IrMDPP(10 wt%) and PVK–PBD(30 wt%)–IrMDPP(10 wt%) in concern [19,20].

complex measured in acetonitrile containing 0.1 M tetrabutylammonium perchlorate with a 100 mV/s scan rate shows an irreversible oxidation onset wave at 0.62 V vs Fc due to oxidation of iridium(III) to iridium(IV), which corresponds to the HOMO energy level. The ligand-based reduction potential corresponding to the LUMO was estimated from the UV–vis absorption edge. The energy diagrams of device ITO/PEDOT/P-Ct–TPD:IrMDPP(0.2–10 wt%)/BCP/Alq$_3$/Mg:Ag/Ag are shown in Fig. 5(b). From the energy levels, hole injection from HOMO of TPD to IrMDPP was easy and electron injection from LUMO of P-Ct to IrMDPP was easy too. Therefore, it demonstrated that the guest partly trapped the hole and electron directly.

On the other hand, the EL spectrum peak was at 595 nm for the device with 10 wt% IrMDPP and it blue shifted to 558 nm when the IrMDPP content decreased to 0.2% in the blends. This is an indication of the decreased interaction among the IrMDPP molecules. The EL spectral data and corresponding CIE coordinate values are presented in Table 1. As the IrMDPP content increased, the color shifts from green-yellow to yellow-orange. In addition, the EL spectra under different voltages were the same, so the device was stable.

The voltage–current density–luminance characteristics and current density–external quantum efficiency–power efficiency characteristics of the LEDs based on blends with IrMDPP content 10 wt% are shown in Fig. 6(a) and (b). The current

Table 1
The CIE coordinates and EL spectral data

IrMDPP (wt%)	CIE(x, y) (at 18 V)	λ (nm, at 18 V)
0.2	0.427, 0.529	558
0.5	0.474, 0.497	571
1.0	0.499, 0.486	575
3.0	0.521, 0.470	580
6.0	0.534, 0.458	586
10.0	0.557, 0.437	595

density is increased with increasing the forward bias and shows typical diode characteristics. The maximum brightness was 3702 cd/m^2 achieved at 25.3 V and maximum current efficiency obtained was 0.83 cd/A.

At the same time, we fabricated the device configuration of ITO/PEDOT/PVK–PBD(30 wt%):IrMDPP(10 wt%)/BCP/Alq$_3$/Mg:Ag/Ag for comparison. Here, PVK is employed as a host due to its high energy blue-emissive singlet-excited state host, its favorable film-forming properties and durability at high temperature, and hole mobility of $\sim 10^{-5}$ cm^2 V^{-1} s^{-1} [16]. PBD was used to facilitate electron transporting and has the same concentration as TPD in P-Ct. Current density and brightness as function of voltage for devices with the structure P-Ct–TPD(30 wt%)–IrMDPP(10 wt%) and PVK–PBD(30 wt%)–IrMDPP(10 wt%) are shown in Fig. 7.
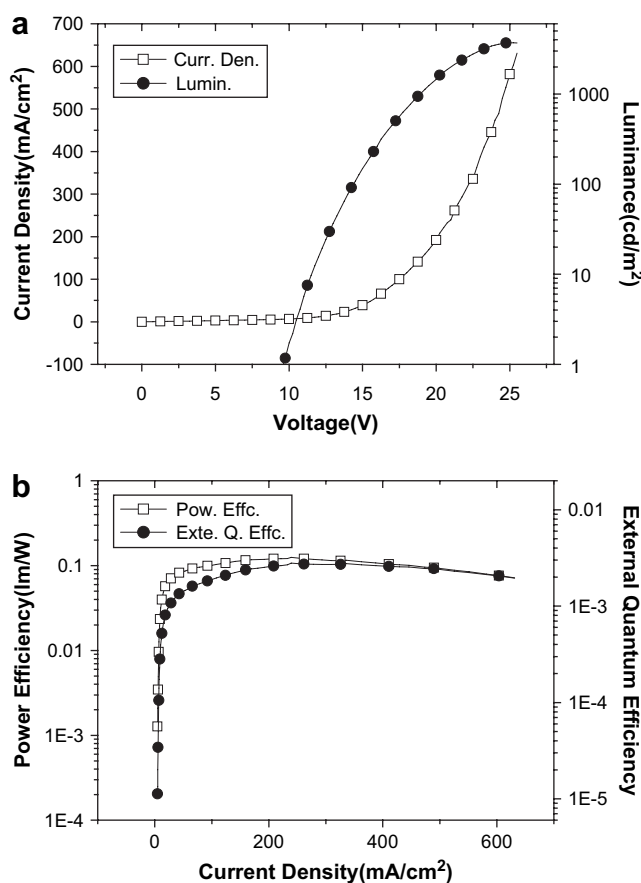

Fig. 6. Performance characteristics of the device with a configuration ITO/PEDOT/P-Ct–TPD:IrMDPP(10 wt%)/BCP/Alq$_3$/Mg:Ag/Ag. (a) Voltage–current density–luminance curves and (b) current density–external quantum efficiency–power efficiency curves.

Compared to the devices with PVK–PBD(30 wt%)–IrMDPP(10 wt%), devices with PCt–TPD(30 wt%)–IrMDPP(10 wt%) exhibit slightly higher current densities. This can be partly explained from the energy levels as shown in Fig. 5(b). The complex constitutes a slightly deeper electron trap in the PBD than in P-Ct [17]. The EL characteristics of LEDs based on IrMDPP doped in PVK–PBD and PCt–TPD host materials are shown in Table 2. It suggests that LEDs based on P-Ct–TPD host material show lower turn-on voltage, much higher brightness, higher external quantum efficiency and power efficiency. As shown in Fig. 5(b), the better electron injection from P-Ct to IrMDPP than PBD and better hole injection from TPD to IrMDPP than PVK which leads to balanced carrier injection and transport and recombination partly explained the better efficiency in device with P-Ct–TPD as host materials. In addition, we investigated the steady and time-resolved photoluminescence with direct excitation of the complex at 315 nm and 298 nm separately as shown in Fig. 8. The transients can be fitted by a bi-exponential function, and there is a decay component with lifetime of 255 ns and 138 ns for the long lived component with blend of P-Ct–TPD–IrMDPP and PVK–PBD–IrMDPP separately. In addition, the PL emission spectra measured under steady-state excitation at an excitation wavelength of 315 nm and 298 nm as shown in Fig. 8(a) revealed that the PL intensity with P-Ct–TPD was much stronger than PVK–PBD. Since the phosphorescence efficiency is approximately proportional to the lifetime [18], the longer lifetime in P-Ct–TPD than in PVK–PBD is consistent with the higher EL efficiencies of the device. Therefore, both the balanced carrier injection and

Fig. 8. (a) PL spectra of P-Ct–TPD(30 wt%)–IrMDPP(10 wt%) and PVK–PBD(30 wt%)–IrMDPP(10 wt%) in the films spin-coated from 10 mg/mL chlorobenzene solution with the same spin rate, excited at 314 nm and 298 nm. (b) Time-resolved PL measurement for P-Ct–TPD(30 wt%)–IrMDPP(10 wt%) and PVK–PBD(30 wt%)–IrMDPP(10 wt%) in the same films.

transport and longer lifetime are attributed to the higher efficiency.

4. Conclusions

In summary, we have compared the concentration dependence of IrMDPP doped in P-Ct–TPD host in PL with EL. The dramatic difference between the EL and PL spectra is an evidence of the dominating role of direct charge trapping and recombination in the EL process over the energy-transfer routes. We have demonstrated higher efficiency in polymer electrophosphorescence using P-Ct–TPD as host materials than using PVK–PBD as host materials with 10 wt% dopant of IrMDPP which was partly due to the more balanced carrier injection and longer lifetime in P-Ct–TPD than in PVK–PBD. P-Ct can be a good choice of host material in polymer electrophosphorescence. In order to design a high-performance PLED, further modification and optimization of the EL devices having P-Ct are in progress.
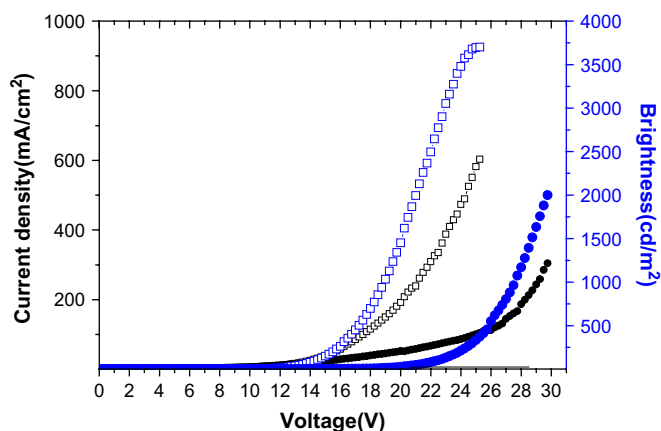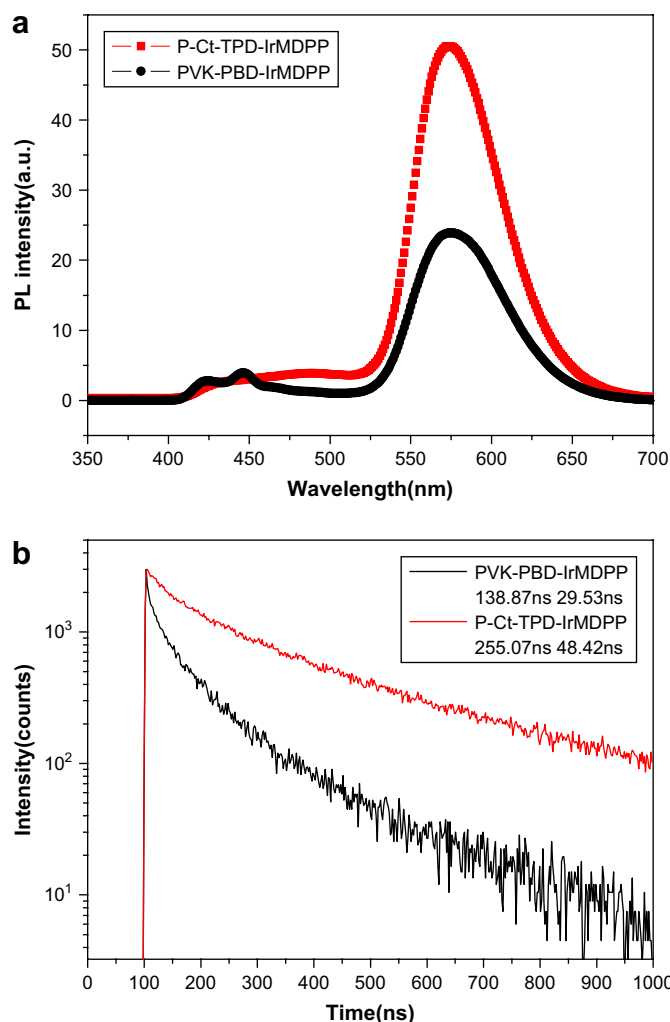

Fig. 7. Current density and brightness as function of voltage for devices with the structure P-Ct–TPD(30 wt%)–IrMDPP(10 wt%) (squares) and PVK–PBD(30 wt%)–IrMDPP(10 wt%) (balls).

Table 2
EL performance of 10 wt% IrMDPP doped in different host polymers (P-Ct and PVK)

Host	V_0/V	L_{max} (cd/m^2)	$\eta_{ext\ max}$ (%)	η_{Lmax} (lm/W)	η_{Imax} (cd/A)
PVK (PBD)	10.5	1999	0.24	0.073	0.68
P-Ct (TPD)	9.7	3702	0.28	0.12	0.83

Acknowledgement

References

[1] Burroughes JH, Bradley DDC, Brown AR, Marks RN, Mackay K, Friend RH, et al. Nature 1990;347:539.

[2] (a) Cao Y, Parker ID, Yu G, Zhang C, Heeger AJ. Nature 1999;397:414;
(b) Wohlgenannt M, Tandon K, Mazumdar S, Ramasesha S, Vardeny ZV. Nature 2001;409:494.

[3] (a) Baldo MA, O'Brien DF, You Y, Shoustikov A, Sibley S, Thompson ME, et al. Nature (London) 1998;395:151;
(b) Baldo MA, Lamansky S, Burrows PE, Thompson ME, Forrest SR. Appl Phys Lett 1998;74:4.

[4] (a) Cleave V, Yahioglu G, Le Barny P, Friend R, Tessler N. Adv Mater 1999;11:285;
(b) Lee CL, Lee KB, Kim JJ. Appl Phys Lett 2000;77:2280;
(c) Cleave V, Yahioglu G, Le Barny P, Hwang DH, Andrew BH, Friend R, et al. Adv Mater 2001;13:44;
(d) Gong X, Ostrowski JC, Bazan GC, Moses D, Heeger AJ. Appl Phys Lett 2002;81:3711;
(e) Shen FZ, Xia H, Zhang CB, Lin D, He L, Ma YG. J Phys Chem B 2004;108:1014.

[5] (a) Baldo MA, Lamansky S, Burrows PE, Thompson ME, Forrest SR. Appl Phys Lett 1999;75:4;
(b) O'Brien DF, Baldo MA, Thompson ME, Forrest SR. Appl Phys Lett 1999;74:442;
(c) Baldo MA, Thompson ME, Forrest SR. Nature 2000;403:750;

[6] (a) Braun D, Heeger AJ. Appl Phys Lett 1991;58:1982;
(b) Suzuki T. J Appl Phys 2006;99:111101;
(c) Friend RH, Gymer RW, Holmes AB, Burroughes JH, Marks RN, Taliani C, et al. Nature 1999;397:121.

[6(d)] Ren XF, Li J, Holmes RJ, Djurovich PI, Forrest SR, Thompson ME. Chem Mater 2004;16:4743.

[7] Shoustikov AA, You Y, Tompson ME. IEEE J Sel Top Quantum Electron 1998;4:3.

[8] Kido J, Hongawa K, Okuyama K, Nagai K. Appl Phys Lett 1993; 63:2627.

[9] Gong X, Robinson MR, Ostrowski JC, Moses D, Bazan GC, Heeger AJ. Adv Mater 2002;14:581.

[10] Kawamura Y, Yanagida S, Forrest SR. J Appl Phys 2002;92:87.

[11] Zhou QF, Li HM, Feng XD. Macromolecules 1987;20:233.

[12] (a) Wang P, Chai CP, Chuai YT, Wang FZ, Chen XF, Fan XH, et al. Polymer 2007;48:5889;
(b) Chai CP, Wang J, Fan XH, Chen XF, Zhou QF. Acta Polym Sin 2006;3:532.

[13] Pope M, Swenberg CE. Electronic processes in organic crystals. Oxford: Clarendon; 1982.

[14] Chao CL, Chen SA. Appl Phys Lett 1998;73:426.

[15] Niu YH, Tung YL, Chi Y, Shu CF, Kim JH, Chen BQ, et al. Chem Mater 2005;17:3532.

[16] Gill WD. J Appl Phys 1972;43:5033.

[17] Yang XH, Jaiser F, Klinger S, Neher D. Appl Phys Lett 2006; 88:021107.

[18] Klessinger M, Michl J. Excited states and photochemistry of organic molecules. New York: VCH; 1995.

[19] Kawamura Y, Yanagida S, Forrest SR. J Appl Phys 2002;80:2045.

[20] Kalinowski J, Stampor W, Virgili D, Fattori V. Chem Phys Lett 2004; 297:39.

[21] (a) Zhang GL, Liu ZH, Guo HQ, Chuai YT, Zou DC. Chem J Chin Univ 2004;3:397;
(b) Lamansky S, Djarovich P, Murphy D, Abdel-Razzaq F, Lee HE, Adachi C, et al. J Am Chem Soc 2001;123:4304.